Chapter 4

Reliability Assessment Considering Wind-Solar-Battery

4.1 Introduction

The reliability analysis enables for a more accurate assessment of the performance of any power system. Some indicators have been suggested in the literature for evaluating the reliability of the electricity supply. These indices are divided into two types: load-based and system-based. When the aging of the sub-components is taken into account, the index values drop [202]. EPDN considers reliability to be a key criterion throughout the design process. As a result, the optimum placement and size of RESs for future reliability assessment have been evaluated. [111] has proposed a restoration method for ENS computation to satisfy the reliability assessment in DS. In [116, 119], the optimization of reliability indices was addressed, and the reliability of the power system was improved.

The literature focuses on the best size and allocation of DGs for improved power system performance. When compared to other approaches, all of the suggested optimization strategies have been shown to be superior. Without considering the effect of optimum DG integration, the system reliability assessment is studied separately. As a result, the PSO for optimum DG placement and size for a 33 bus distribution system is presented. Simultaneously, the parameters listed in Table 2.5, which have not been addressed before, are taken into account. The optimization technique's competitiveness is shown by comparisons with other prior methods. Integrating the one, two, and three distributed sources in 33 bus DS yields a comparative analysis for the decrease of electrical power loss and voltage deviation. After that, the findings are

compared to the existing literature. The reliability assessment is completed after the power loss has been minimized and the bus voltages have been enhanced. After the system's reliability assessment is completed with and without the integration of DG, the performance analysis is completed for selected DSs.

The reliability assessment in the DS is an emerging area of research. Thus, the chapter mainly focuses on the reliability assessment of DSs. For the accomplishment of the above task, a work flowchart is framed in Figure 4.1.

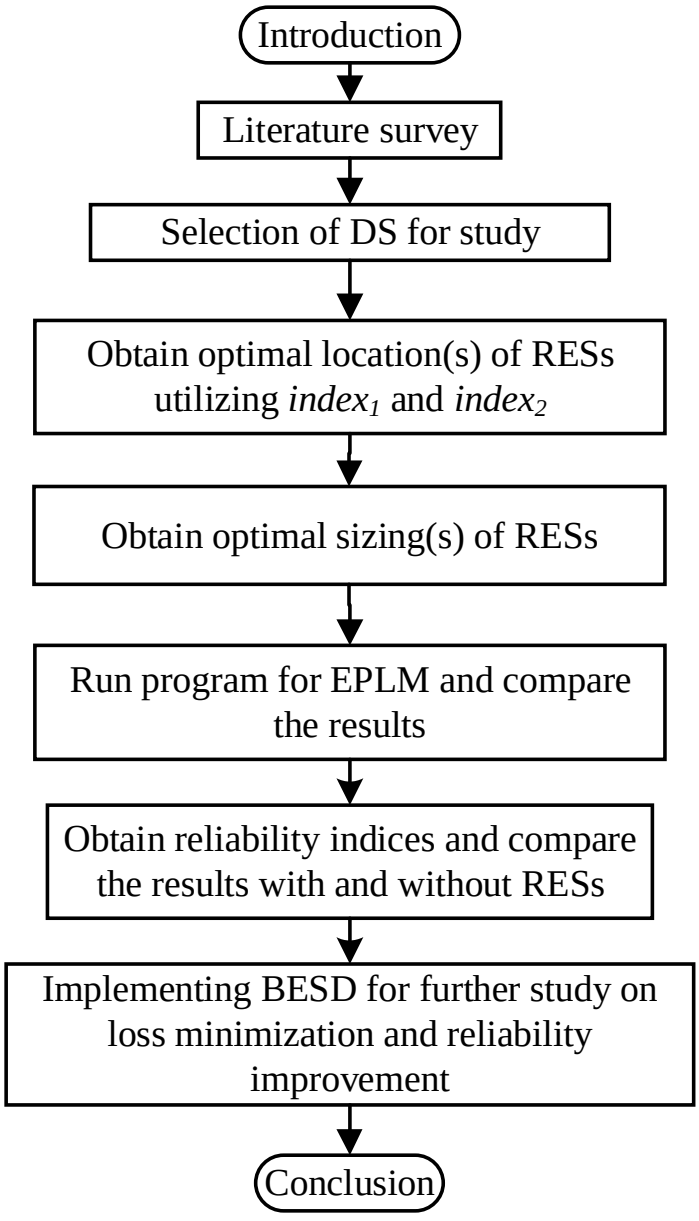

Figure 4.1: Flow chart of research work performed in this chapter.

4.2 Problem Formulation

The bus voltage and system reliability are the most affecting factors for the EPDN when losses are considered. It becomes necessary to improve these two factors by implementing Distributed Generation (DG) into the EPDN. DG siting is one of the favored techniques used in the EPDN for the improvement of the system's reliability and bus voltage profile, including EPLM. The DG location, DG size, DG pf, DG penetration, and DG type are required for the effective implementation of DGs in the EPDN. Simultaneously, it is required to study the mathematical expressions, and modeling of related parameters and DGs integrated into the system. An overview of parameters considered for the EPLM and mathematical modeling are elaborated in the upcoming subsections.

4.2.1 Optimal Location

Obtaining the optimal location of DGs is crucial part of EPDN. To identify the optimal locations, two indexes are proposed. The $index_1$ is implemented only for placing the single DG and $index_2$ is incorporated for placing more than one DGs in the EPDN. Power loss is minimized by using $index_1$ for placing 1DG (viz. the Case 1). However, $index_2$ provides minimum power loss for multiple DGs (viz. Case 2 and Case 3). These two indexes are represented by Equations (4.17) and (4.22), respectively. It can be observed from the equation of $index_1$ that the large index value depicts the weakest node of the system because the complex power injected at bus i is large. It implies that the single DG can be placed at this particular bus. On the other hand, $index_2$ shows the voltage stability, which concludes that the reduced values of this index give the weakest bus of the EPDN. Table 4.1 shows the values of both the indexes with corresponding five buses to arrange DG optimally in a given EPDN. Therefore, DGs can be placed hierarchically at these buses.

In Figure 4.2, V_a and V_b are the magnitudes of the voltages at buses a and b, respectively. δ_a and δ_b are the phase angles of the voltages at buses a and b, respectively. Z_l and Y_l are the impedance and admittance of l-line, respectively. R_l and X_l are the resistance and reactance of a l-line. I_l is the current in the l-line. The electrical power loss in the l-line is given by Equation (4.1).

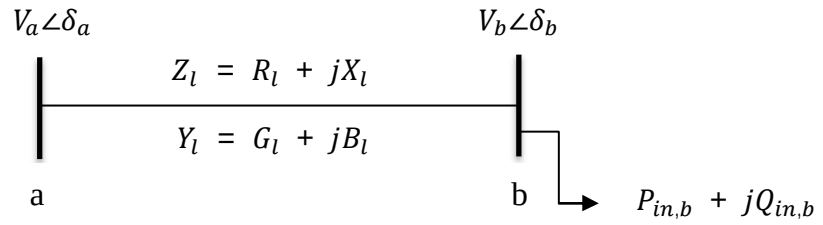

Figure 4.2: General 2-bus system to formulate the line loss and load factor.

$$S_{LOSS_l} = (V_a - V_b) \times I_l^* \tag{4.1}$$

$$I_l = (V_a - V_b) \times Y_l \tag{4.2}$$

Then the bus voltage matrix is formed by using Equation (4.3) Where

Z_{bus} is the network impedance matrix

I_{bus} is the bus injection matrix

- n_{bus} is the number of total buses in EPDN

$$[V_{bus}]_{n_{bus}\times 1} = [Z_{bus}]_{n_{bus}\times n_{bus}}[I_{bus}]_{n_{bus}\times 1} \tag{4.3}$$

By expanding Equation (4.3), the node voltages can be obtained by using Equations (4.4) and (4.5).

$$V_a = \sum_{i=1}^{n_{bus}} Z_{ai} \times I_i \tag{4.4}$$

$$V_b = \sum_{i=1}^{n_{bus}} Z_{bi} \times I_i \tag{4.5}$$

Where

- *i* is 1,2,. . . ,n_{bus}
- Z_{ai}, Z_{bi} and I_i are the element of impedance matrix that signify the a_{th} row and i_{th} column, b_{th} row and i_{th} column, and current injection at bus-i, respectively.

$$\text{Current Injection}, I_i = \frac{(P_{in,i} + jQ_{in,i})^*}{V_i^*} \tag{4.6}$$

Where

- $P_{in,i}$ and $jQ_{in,i}$ are active power and reactive power injected at bus-i, respectively
- V_i^* is the voltage at bus-i

Now, put Equation (4.2) and Equations (4.4)–(4.6) in Equation (4.1) then the electrical loss of the line-l is derived as Equation (4.7).

$$S_{LOSS,l} = [V_a - V_b]\left(\frac{\sum^{n_{bus}}(Z_{ai} - Z_{bi})Y_l}{V_i^*}\right)^* [P_{in,i} + jQ_{in,i}] \tag{4.7}$$

For an electrical system with n_l number of branch/lines, the line loss is given by Equation (4.8).

$$[B_{LOSS_l}] = \sum_{i=1}^{n_{bus}} \frac{(V_a - V_b)(Z_{ai} - Z_{bi})^* Y_l^*}{V_i} S_{in,i} \tag{4.8}$$

Where B_{LOSS_l} is line loss, $S_{in,i}$ is apparent power injected at bus-i, l is 1 to n_l.

$$[B_{LOSS_l}] = \sum_{i=1}^{n_{bus}} [LF_{li}][S_{in,i}] \tag{4.9}$$

$$LF_{li} = \sum_{i=1}^{n_{bus}} \frac{(V_a - V_b)(Z_{ai} - Z_{bi})^* Y_l^*}{V_i} \tag{4.10}$$

$$LF_{li} = \begin{cases} \text{non-zero}, & \text{if l-line is in the path of bus-i} \\ 0, & \text{Else} \end{cases} \tag{4.11}$$

Where load factor (LF) is given by $\frac{(V_a - V_b)(Z_{ai} - Z_{bi})^* Y_l^*}{V_i}$. LF_{li} is load factor of the lth line due to the ith bus injection (it is non-zero if lth line is in the path of ith bus else zero) as described in Equation (4.11). For example, a 6-bus distribution is taken for explanation and a general branch loss formula is derived as Equation (4.12).

$$\begin{bmatrix} B_{LOSS_1} \\ B_{LOSS_2} \\ B_{LOSS_3} \\ B_{LOSS_4} \\ B_{LOSS_5} \end{bmatrix}_{5\times1} = \begin{bmatrix} LF_{11} & LF_{12} & LF_{13} & LF_{14} & LF_{15} & LF_{16} \\ LF_{21} & LF_{22} & LF_{23} & LF_{24} & LF_{25} & LF_{26} \\ LF_{31} & LF_{32} & LF_{33} & LF_{34} & LF_{35} & LF_{36} \\ LF_{41} & LF_{42} & LF_{43} & LF_{44} & LF_{45} & LF_{46} \\ LF_{51} & LF_{52} & LF_{53} & LF_{54} & LF_{55} & LF_{56} \end{bmatrix}_{5\times6} \times \begin{bmatrix} S_{in_1} \\ S_{in_2} \\ S_{in_3} \\ S_{in_4} \\ S_{in_5} \\ S_{in_6} \end{bmatrix}_{6\times1} \tag{4.12}$$

$$[B_{LOSS}M]_{5\times1} = [LFM]_{5\times6} \times [S_{in}M]_{6\times1} \tag{4.13}$$

Where

- $[B_{LOSS}M]$ is branch/line loss matrix
- $[LFM]$ is the load factor matrix
- $[S_{in}M]$ is complex power injection matrix

Equation (4.13) is reduced accordingly. Where power injection at all the buses except the source bus are available.

$$\begin{bmatrix} B_{LOSS_1} \\ B_{LOSS_2} \\ B_{LOSS_3} \\ B_{LOSS_4} \\ B_{LOSS_5} \end{bmatrix}_{5\times1} = \begin{bmatrix} 0 & LF_{12} & LF_{13} & LF_{14} & LF_{15} & LF_{16} \\ 0 & 0 & LF_{23} & LF_{24} & LF_{25} & LF_{26} \\ 0 & 0 & 0 & LF_{34} & LF_{35} & 0 \\ 0 & 0 & 0 & 0 & LF_{45} & 0 \\ 0 & 0 & 0 & 0 & 0 & LF_{56} \end{bmatrix}_{5\times6} \times \begin{bmatrix} S_{in_1} \\ S_{in_2} \\ S_{in_3} \\ S_{in_4} \\ S_{in_5} \\ S_{in_6} \end{bmatrix}_{6\times1} \tag{4.14}$$

$$A_i = \sum_{l=1}^{n_l} LF_{li} \tag{4.15}$$

The calculation of effective power injections is performed, as given in Equation (4.16).

$$\left.\begin{aligned} S_{eff,6} &= S_{in,6} \\ S_{eff,5} &= S_{in,5} \\ S_{eff,4} &= S_{in,4} + S_{eff,5} \\ S_{eff,3} &= S_{in,3} + S_{eff,4} + S_{eff,6} \\ S_{eff,2} &= S_{in,2} + S_{eff,3} \\ S_{eff,1} &= S_{in,1} + S_{eff,2} \end{aligned}\right\} \tag{4.16}$$

Equation (4.17) shows the final equation for the calculation of $index_1$. The index is implemented for attaining the optimal position of one energy source as conventional generation. In Equation (4.15), $|A_i|$ is fully dependent on LF values of all the branches (or lines) connected between bus and the source bus (main station). The closeness of the i_{th} bus from the source bus can be observed in the LF_{li}, as guided in Equation (4.10). If the i_{th} bus is not near, the number of lines between i_{th} bus and source bus is being plenty and the corresponding Z_{ai}, Z_{bi}, and Y_l parameters will account in the electrical loss component. Furthermore, if the node voltage is high, the value of LF_{li} will be small and vice-versa as observed in the derived equation. The equation of $index_1$ is also accounted for the effective complex power supplied by the i_{th} bus. The $index_1$ will be high only when both the terms are high in Equation (4.17). Thus, the value

of $index_1$ represents its main contribution in the total electrical loss and hence, in finding the optimal siting of one conventional generation.

$$(index_1)_i = |A_i| \times |S_{in_{eff_i}}| \tag{4.17}$$

$S_{in_{eff_i}}$ is the effective injection of complex power, which is the sum of injected powers from other buses connected to ith bus.

Refer Figure 4.2,

$$I_l = \frac{V_a - V_b}{R_l - jX_l} \tag{4.18}$$

$$P_{in,b} - jQ_{in,b} = V_b{}^* I_l \tag{4.19}$$

Solving Equations (4.18) and (4.19),

$$|V_b|^4 - b_l|V_b|^2 + c_l = 0 \tag{4.20}$$

Where

- b_l = $|V_a|^2$ - $2P_{in,b}R_l$ - $2Q_{in,b}X_l$
- c_l = $(P_{in,b}^2 + Q_{in,b}^2)(R_l^2 + X_l^2)$

Solving Equation (4.20) for the possible solution, we get

$$|V_b| = 0.707\{b_l + (b_l^2 - 4c_l)^{\frac{1}{2}}\}^{\frac{1}{2}} \tag{4.21}$$

After the simplification of Equation (4.21), we get $index_2$ as given in Equation (4.22).

$$(index_2)_{a+1} = |V_a|^4 - 4(P_{in,b}X_l - Q_{in,b}R_l)^2 - 4(P_{in,b}R_l - Q_{in,b}X_l)|V_a|^2 \tag{4.22}$$

Where

- l refers branch number
- a = 1, 2,. . . , n_{bus}

$index_2 \geq 0$ for stable operation of distribution network functioning. This index may be used to determine the degree of stability; therefore, the bus with the lowest index value implies that the bus is more vulnerable to voltage collapse. The values obtained for $index_1$ and $index_2$ are mentioned in Tables C.1 and C.2, respectively in Appendix C.

Table 4.1: Values of indexes with corresponding bus number

$index_1$		$index_2$	
Value	**Bus No.**	**Value**	**Bus No.**
1.349×10^{-3}	6	41.52×10^{-3}	30
0.928×10^{-3}	29	16.44×10^{-3}	13
0.871×10^{-3}	30	16.43×10^{-3}	24
0.866×10^{-3}	5	7.36×10^{-3}	31
0.856×10^{-3}	28	6.49×10^{-3}	20

4.2.2 Power balance

The active power and reactive power balance expressions are shown in Equations (4.23) and (4.24).

$$P_{net_i} = P_{dg_i} - P_{dem_i} - V_i \sum_{j=1}^{N_{bus}} V_j Y_{i,j} cos(\delta_i - \delta_j - \theta_i + \theta_j) \tag{4.23}$$

$$Q_{net_i} = Q_{dg_i} - Q_{dem_i} - V_i \sum_{j=1}^{N_{bus}} V_j Y_{i,j} sin(\delta_i - \delta_j - \theta_i + \theta_j) \tag{4.24}$$

Where

- P_{net_i} = 0 and Q_{net_i} = 0 are the net active power and reactive power at i-bus, respectively
- P_{dg_i} and Q_{dg_i} represent DG active power and reactive power at i-bus, respectively
- Active and reactive load demands are mentioned by P_{dem_i} and Q_{dem_i}, respectively
- V_j is the bus voltage at j-bus, $Y_{i,j}$ is the branch admittance between i, j-buses
- δ_i and δ_j represent the phase angles of i-bus and j-bus voltages, respectively
- $(\theta_i - \theta_j)$ are the impedance angle of branch connected between i and j-buses

4.2.3 Objective Function

In this research the objective function is considered to be active power loss minimization in the EPDN. The reliability indices are then evaluated by fixing the optimal location and size of the DGs. The objective function of the problem is given in Equation (4.25).

A. Active Power Loss

The minimization of active power loss occurred in EPDN is the objective function considered. The primary aim of the Optimal Power Flow technique is to minimize the system active power loss as given as Equation (4.25).

$$\min AP_{loss} = \sum_{i=1}^{N_{bus}} \sum_{j=1}^{N_{bus}} C_{1_{ij}}(P_{real_i}P_{real_j} + Q_{real_i}Q_{real_j}) + C_{2_{ij}}(Q_{real_i}P_{real_j} - P_{real_i}Q_{real_j}) \tag{4.25}$$

Where

- $P_{real_i}, P_{real_j}, Q_{real_i}, Q_{real_j}$ are the active power and reactive power at *i* and *j*-buses, respectively
- N_{bus} is the number of buses or nodes

$C_{1_{ij}}$ and $C_{2_{ij}}$ are defined as follows.

$$C_{1_{ij}} = \frac{R_{ij}}{V_i V_j} cos(\delta_i - \delta_j) \tag{4.26a}$$

$$C_{2_{ij}} = \frac{R_{ij}}{V_i V_j} sin(\delta_i - \delta_j) \tag{4.26b}$$

Where

- V_i, δ_i and V_j, δ_j are the voltages and corresponding angles at ith and jth buses, respectively
- R_{ij} is the resistance of a branch between i and j-buses

B. Reactive Power Loss

The availability of reactive power ensures the active power transmission from source to load. Voltage stability margin or bus voltages are also dependent on this reactive power support. The reactive power loss is obtained at different pf of DG using Equation (4.27).

$$RP_{loss} = \sum_{i=1}^{N_{bus}} Q_{gen_i} - \sum_{i=1}^{N_{bus}} Q_{dem_i} \tag{4.27}$$

Where

- Q_{gen_i} and Q_{dem_i} are the reactive power generation and demand at the ith bus (including the slack bus), respectively
- Q_{dem_i} is reactive power demand at the ith bus

4.2.4 Reliability Indices

The indices are assessed for divergent DG reliability data by fixing the site and size of DGs. Furthermore, the reliability improvement of distribution network has been accomplished by integrating one DG and multiple DGs in the EPDN. Several reliability indices exist to observe the system's reliability such as EENS, AENS, SAIDI, SAIFI, and ASAI which are also used in this study to analyze the reliability improvement. The indices of the network reliability are dependent function of failure rate (λ_p) and Repair Time as given in Equation (4.28) [7,116,119].

$$\text{Reliability Indices} = f(\lambda_p, RT) \tag{4.28}$$

4.2.5 Constraints

The objective function minimization is a primary task to obtain the optimal results. Objective function minimization is subjected to design the constraints so that the requirements of the EPDN must be satisfied with DG operation. Thus, the constraints are discussed in the succeeding subsection [203, 204].

A. Equality Constraints

These constraints follow the Kirchhoff's current rule as the algebraic sum of powers in and powers out should be equal in an EPDN [204, 205]. Two of these constraints are described as follows.

$$\sum_{i=1}^{N_{bus}} AP_{gen_i} = \sum_{i=1}^{N_{bus}} AP_{dem_i} + AP_{loss} \tag{4.29}$$

Where

- AP_{gen_i} is active power generated by the generation units at ith bus
- AP_{dem_i} is active power demand at ith bus

$$\sum_{i=1}^{N_{bus}} RP_{gen_i} = \sum_{i=1}^{N_{bus}} RP_{dem_i} + RP_{loss} \tag{4.30}$$

Where

- RP_{gen_i} is reactive power generated by the generation units at ith bus
- RP_{dem_i} is reactive power demand at ith bus

B. Inequality Constraints

These constraints are associated with the limits applied to the system parameters for the operation of EPDN. Some of these constraints are described as follows.

(a) Power flow

To maintain the line capacity within limits, these constraints ensure the apparent power to be within limits at the ends of a line [203, 204].

$$AP_{a_{ij}} \leq AP_{a_{ij}}^{max} \tag{4.31}$$

Where

- $AP_{a_{ij}}^{max}$ is the highest permissible apparent powers (AP_a) for lines i to j
- $AP_{a_{ij}}$ is the actual AP_a transmitted from i to j

(b) DG capacity

These limits ensure the non-reversal of power flow. The power from the substation is provided to the EPDN must be greater than the DG power. Also, the DG has the minimum and maximum power generation boundaries [206].

$$\sum_{i=1}^{n_{DG}} AP_{DG_i} \leq \sum_{i=1}^{n_{bus}} AP_{dem_i} + AP_{loss} \tag{4.32}$$

$$\sum_{i=1}^{n_{DG}} RP_{DG_i} \leq \sum_{i=1}^{n_{bus}} RP_{dem_i} + RP_{loss} \tag{4.33}$$

$$AP_{DG_p}^{min} \leq AP_{DG_p} \leq AP_{DG_p}^{max} \tag{4.34}$$

$$RP_{DG_p}^{min} \leq RP_{DG_p} \leq RP_{DG_p}^{max} \tag{4.35}$$

Where

- p = 1, 2,. . . . . , n_{DG}
- $AP_{DG_p}^{min}$ (set to zero) and $AP_{DG_p}^{max}$ (from Equation ((4.32))) are the lower and upper *AP* outputs of *DG* unit p, respectively

- $RP_{DG_p}^{min}$ (set to zero) and $RP_{DG_p}^{max}$ (from Equation ((4.33))) are the lower and upper *RP* outputs of *DG* unit p, respectively

- n_{DG} is the number of DGs present in the distribution network

(c) Bus voltage

The voltages at buses present in the EPDN must be limited within minimum and maximum limits [207, 208].

$$|V_{i_{minimum}}| \leq |V_i| \leq |V_{i_{maximum}}| \tag{4.36}$$

Where

- $|V_{i_{minimum}}|$ and $|V_{i_{maximum}}|$ is the lower and upper boundaries of the bus voltage $|V_i|$ which are set to 95% and 105%, respectively.

(d) Branch current

It refers as thermal capacity of the EPDN lines. The current in the distribution lines must be within limits and should exceed the maximum current as given in Equation (4.37) [116].

$$I_i \leq I_i^{max} \tag{4.37}$$

4.2.6 Constriction Factor-based Particle Swarm Optimization Technique

PSO is a novel progression computational technique which is in the frame since 1995. The use of this method is seen in reactive power dispatch [209], generation scheduling [210], renewable source integrated power system [211], and cost analysis [212]. In basic PSO method, the candidate solution is improved iteratively under any given constraint. The PSO algorithm is shown in Figure 4.3. Due to the reduction in computational time and requirement of less memory, PSO has overtaken many algorithms including the Genetic algorithm (GA) as PSO is mutation free. It searches the optimized value globally with the help of several particles present in a swarm based on specific constraints. As all particles have its local and global best values because of its own and global positions. This method updates the particle position and velocity as described in Equations (4.38) and (4.39).

$$V_n^{p+1} = W' \times V_n^p + C_1' \times R_1' \times (Personal_{BEST_i} - X_n^p) + C_2' \times R_2' \times (Global_{BEST} - X_n^p) \tag{4.38}$$

$$X_n^{p+1} = X_n^p + C_f \times V_n^{p+1} \tag{4.39}$$

Where V_n^{p+1} = n^{th} particle velocity at $(p+1)^{th}$ iteration, W' = particle inertial weight, V_n^p = n^{th} particle velocity at p^{th} iteration, C_1', C_2' = constants (0, 2.5), R_1', R_2' = numbers generated randomly (0, 1), $Personal_{BEST_i}$ = the n^{th} particle's best position considering its own property, $Global_{BEST}$ = the n^{th} particle's best position considering the whole population, X_n^{p+1}, X_n^p = n^{th} particle position at $(p+1)^{th}$ and p^{th} iterations, respectively. C_f = Constriction Factor assures efficient convergence [213, 214].

Due to faster convergence to the global point, the basic PSO faces the difficulty of premature convergence. The particles have started oscillating around the optimal point without providing any type of restriction to the highest velocity of the particles available in swarm. Therefore, the optimal global solution is rare to obtain. The use of properly defined Constriction Factor is briefly described for advance convergence of the PSO [215]. This can also be applied for the DG siting and DG size in the EPDN. It reduces the computation time and requires little memory. Although this technique suffers from partial optimization, by altering its parameter during problem solving will produce an improved result [216–218]. To obtain the improved result, a Constriction Factor is used and thus, the method is known as CF-PSO technique. The parameters set for the CF-PSO are as follows. The values of initial weight, final weight, C_1, C_2, R_1, R_2, and Constriction Factor are considered to be 9×10^{-1}, 4×10^{-1}, 201×10^{-2}, 201×10^{-2}, 0 to 1, 0 to 1, and 729×10^{-3}, respectively. A flowchart is provided in Figure 4.3 to obtain the DG location, DG sizing and system reliability of the DGs in 33 bus EPDN.

4.3 Power Equations of Renewable Energy Sources

The reliability assessment of the IEEE 33 bus EPDN is accomplished, considering the optimal siting(s) and sizing(s) of SPV, WTG, and BESD. In this regard, a brief modeling and specifications of these RESs are illustrated.

4.3.1 Wind Turbine Generator

The V162-5.6MW(IECS based on IEC IIB), a WTG, manufactured by General Electric Company is considered for its output power rating. The specifications of the WTG considered in

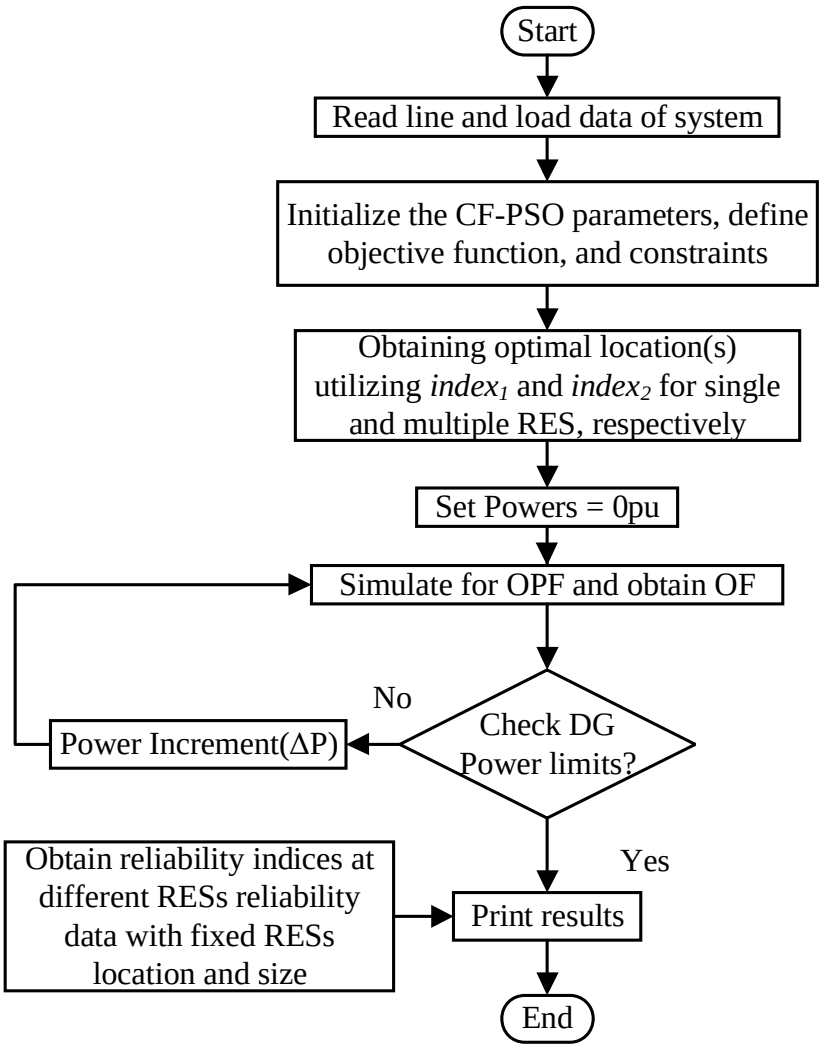

Figure 4.3: Algorithm implemented for the research work.

this study are provided in Table 4.2. The mechanical power of WTG (P_{mech}) is a function of generator rotor speed and wind speed as formulated in Equations (4.40) and (4.41) [219].

$$P_{mech}(v_{wind}, \omega_{rotor}) = \frac{1}{2} \times \rho \times v_{wind}^3 \times C_p(\lambda, \theta) \tag{4.40}$$

Where

- ρ is air density
- A_s is area swept by the turbine rotor blades
- $Vwind$ is speed of the wind
- C_p is the non-linear function of the tip speed ratio (λ) and pitch angle (θ)
- ω_{rotor} is generator rotor speed

$$P_{WTG} = \begin{cases} 0; & 0 \leq V \leq V_{cin} \text{or} V \geq V_{cout} \\ P_{WTG,rated} \times \left(\frac{V - V_{cin}}{V_{rated} - V_{cin}} \right); & V_{cin} \leq V \leq V_{rated} \\ P_{WTG,rated}; & V_{rated} \leq V \leq V_{cout} \end{cases} \tag{4.41}$$

Where

- P_{WTG} is output WTG power
- $P_{WTG,rated}$ is rated output WTG power
- V_{rated} is rated wind speed

Table 4.2: Wind Turbine (V162-5.6 MW) specifications

Parameter	**Rating (Unit)**
Rated output power	5.6 MW
Cut-in Speed (V_{cin})	3 m/s
Cut-out Speed (V_{cout})	25 m/s
Temperature	-20 °C to 45 °C
Diameter	162 m
Swept Area	20612 m^2
Frequency	50/60 Hz
Hub Height	119 m (min) and 166 m (max)

4.3.2 Solar Photovoltaic

The Surface Plasmon Resonance (SPR)-P5-545-UPP, a Solar PV Module, manufactured by Sunpower Company is considered for its output power rating. The specifications of the SPV module considered in this study are provided in Table 4.3. The SPV module is developed by implementing several cells. The power output for the SPV module can be derived as described by Equations (4.42) and (4.43) [220–222].

$$P_{SPV(AC)}(t) = P_{SPV(out)}(t) \times \eta_{inverter} \tag{4.42}$$

$$P_{SPV(out)}(t) = FF_A(t) \times I_{short}(t) \times V_{open}(t) \tag{4.43}$$

Where

- t = time instant
- $P_{SPV(AC)}(t)$ = AC output power
- $P_{SPV(out)}(t)$ = maximum output power
- $\eta_{inverter}$ = inverter efficiency
- $FF_A(t)$ = fill factor actual
- $I_{short}(t)$ = short circuit current under operating conditions
- $V_{open}(t)$ = open circuit voltage under operating conditions

Table 4.3: Bifacial Solar Panel (SPR-P5-545-UPP) specifications

Parameter	**Rating (Unit)**	**Parameter**	**Rating (Unit)**
Nominal power	545 W	Maximum Series Fuse	25 A
Tolerance of Power	$\pm 3/0\%$	Temperature	-40°C–85°C
Efficiency	21.1%	Power Temperature Coefficient	-0.34%/°C
Rated voltage	46.1 V	Voltage Temperature Coefficient	-0.28%/°C
Rated current	11.84 A	Current Temperature Coefficient	0.06%/°C
Open circuit voltage	55.8 V	Weight	31.5 kg
Short circuit current	12.62 A	Solar Cells	Mono-crystalline
Maximum System Voltage (IEC)	1500 V	L × B × H mm^3	2362 × 1092 × 35

4.3.3 Battery Energy Storage Device

The BESD-BESS 3000, a Lithium-Ion Battery System, manufactured by Freqcon Company is considered for its output power rating. The specifications of the BESD considered in this study are provided in Table 4.4. Mathematical modeling has been describes further. The BESD dispatch strategy starts functioning by monitoring the peak load hours. If the peak load is greater/less than the capacity of WTG and SPV, the BESD discharges/charges to support the distribution network; otherwise the BESD operates as a neutral device. Also, the BESD SOC will decide the charging or neutral operation during the off-peak hours. The battery model is

derived with the help of Equations (4.44) and (4.45) assuming that no battery is self-discharging [223].

$$P_{Battery(DC)}(t) = \frac{E_{Battery}(t) - E_{Battery}(t - \Delta t)}{\Delta t} \tag{4.44}$$

$$P_{Battery(AC)}(t) = \begin{cases} \frac{P_{Battery(DC)}(t)}{\eta_{Battery}}; P_{Battery(DC)}(t) > 0 \\ P_{Battery(DC)}(t) \times \eta_{Battery} \times PF_{Inverter}; Otherwise \end{cases} \tag{4.45}$$

Where

- $P_{Battery(DC)}(t)$ = DC charging/discharging power of the battery in Δt interval (W)
- $E_{Battery}(t)$ = energy of battery (Wh)
- $P_{Battery(AC)}(t)$ = AC power discharged/charged state of battery
- $\eta_{Battery}$ = efficiency of the battery
- $PF_{Inverter}$ = inverter power factor

Table 4.4: BESD (BESS 3000) specifications

Parameter	**Rating**
Rated output power	3000 kW
Storage Capacity	1000 kWh
Rated output current	2795 A
Rated output AC voltage	620 V
Power factor	0.95 Cap . . . 0.95 Ind
Total harmonic distortion	$<3\%$
Efficiency	$>98\%$
Type	Lithium-ion
IGBT Switching Frequency (Converter)	2–4 kHz

4.4 Results and Discussion

The DG location, DG size, and EPDN reliability are obtained and analyzed. The 33 bus EPDN (Figure A.1 of Appendix A is considered. The branch and load data for this EPDN are adopted

from [224]. It contains 33 buses and 32-branches with a total of 3.715 MW and 2.3 MVar active power and reactive power loads, respectively. This EPDN operates at 12.66 kV, 100 MVA base values. The active power loss and reactive power loss for without DG case are obtained as 0.211009 MW and 0.143056 MVar, respectively. The objective function minimization is performed by implementing the CF-PSO, as explained. The following steps are followed to obtain the results.

- **Step 1:** Optimal siting(s) and sizing(s) of WTG, SPV, and BESD are evaluated considering electrical loss minimization (ELM). The technical ratings of WTG, SPV, and BESD have been illustrated in Tables 4.2–4.4, respectively. The BESD is assumed to be fully charged and produces its rated output power.

- **Step 2:** Active power loss, reactive power loss, and bus voltages are obtained by integrating WTG, WTG+SPV, and WTG+SPV
  +BESD (referred as Case 1, Case 2, and Case 3, respectively) in the EPDN to analyze the results obtained in Step 1.

- **Step 3:** Reliability indices are estimated for EPDN considering two different WTG and SPV reliability data, including λ_p and RT (for Scenario 1 to Scenario 6).

- **Step 4:** Furthermore, the reliability improvement is analyzed by adding BESD (considering 100% reliable) to the EPDN in the presence of WTG and SPV. All related reliability data used are mentioned in Table 1.1. Load distribution and classification for 33 bus DS have been taken from Tables B.2 and B.4, as provided in Appendix B.

4.4.1 Renewable Energy Source: Location and Rating

The bus number is obtained to allocate WTG, SPV, and BESD. The two indexes are implemented to obtain the locations as described. It is observed from the analysis that $index_1$ provides the location suitable for a single DG. This index examines the effective apparent power injection to the buses. The Load Factor value of lth line depends on whether the lth is in the path of the ith bus to the source node or not. The multiplication of Load Factor and injected apparent power provides the active power loss and reactive power loss of lth line due to the ith bus AP_a injection. Thus, the maximum value of $index_1$ at ith bus indicates the candidate bus

to place one DG. The first six values of this index for respective buses are provided in Table 4.1.

The optimal siting for several DGs are found by implementing the $index_2$. This index provides the hierarchy of weak buses in the EPDN. It shows the sensitivity of the bus towards voltage collapse. The value of $index_2$ must be greater than or equals to zero for ensuring the stable operation of the distribution network. The minimum value of this index depicts more sensitivity to the voltage collapse and thus, referred to as the weak bus. The optimal location(s) and size(s) of WTG, SPV, and BESD for three cases are obtained and reproduced in Table 4.5. The DGs are accommodated according to the locations obtained from the indexes, as mentioned in this chapter. The DG size and minimum active power loss are then evaluated, implementing CF-PSO, as described earlier.

Table 4.5: DG location and DG size obtained

Parameter	**Case 1**	**Case 2**	**Case 3**
Location (bus no.)	6	30, 13	30, 13, 24
size@UPF (MW)	2.564	1.148, 0.843	1.048, 0.801, 1.105

4.4.2 Active and Reactive Power Loss, and Bus Voltage

The accommodation of DG at an optimal location with optimal size reflects in voltage profile improvement and minimization of active power loss and reactive power loss. Most of the research has concentrated on active power loss minimization because of the dominance of I^2R losses in the EPDN. In contrast, the reactive power loss minimization for overall voltage improvement of all the 32 buses of the EPDN has also been observed. The estimation of active power loss, reactive power loss, and voltage profile is considered before analyzing the system's reliability. This is performed to analyze the system's reliability with the optimal DG size, DG location, minimum power loss, and better bus voltages. Several kinds of research are performed to obtain active power loss minimization, which is cited in Table 4.6 for single and multiple DGs, respectively. It is observed from Table 4.6 that the authors of the mentioned literature have not dealt with the cases considering various DGs combination. Therefore, it is vital to observe that the results obtained considering several types of DGs are compared with the conventional DGs [225]. The output results obtained for the active power loss are tabulated in Table

Table 4.6: Literature results related to IEEE 33 bus with multiple DGs

Method	# of DG	DG Position	Total DG Size (MW)	Loss (MW)	Reference
MOGA	1(SPV)	8	1.6333	0.113	[127]
	2(SPV)	14, 30	0.8337, 0.99851	0.08435	
	1(WTG)	8	1.85	0.08556	
	2(WTG)	14, 30	1.1, 0.75	0.04791	
GA	3(SPV)	14, 24, 28	0.6947, 1.1844, 1.4628	0.0756	[16]
ABC	3(SPV)	9, 24, 32	1.1372, 1.0674, 0.8031	0.0752	
PSO	3(SPV)	9, 24, 30	1.0625, 1.0447, 0.9518	0.0744	
BBO	3(SPV)	14, 24, 30	0.7539, 1.0994, 1.0714	0.0715	
CSO	5(BESD)	1, 4, 11, 12, 18	0.15, 0.4117, 0.6705, 0.1, 8.9055	0.02379	[124]
DMA	1(SPV)	6	2	0.0908	[129]
		18	1	0.1175	
	1(WTG)	33	1.65	0.1068	

4.7. This table shows that the active power loss value is better for Case 1, and comparable for Case 2 and Case 3. The slight variations in active power loss for Case 2 and Case 3 are observed because the authors have considered the pf of WTG only. Furthermore, the bus voltages with one DG and multiple DGs is drawn in Figure 4.4. The voltages at all the buses vary according to the active power loss and reactive power loss in the electrical system. Therefore, the system requires real power support for active power loss minimization, which improves the bus voltages by compensating the I^2R losses. Furthermore, it is concluded from Table 4.7 that the active power loss minimization is not reduced significantly for Case 3 as compared to Case 2. Thus, there is a marginal improvement in bus voltage profile for Case 3 as compared to Case 2, which is depicted in Figure 4.4. Also, the improvement in bus voltages is observed when multiple DGs are placed. This voltage profile is further improved at 0.85 and 0.82 pfs. This is because of increment in reactive power support at system buses. It is the point of interest to know about the two voltage peaks when the system is operated with single DG. The two voltage peaks appear at bus number 7 and 26 because these buses are directly connected to bus 6, at which single DG is placed optimally. Also, the size of the single DG is greater than the sum of the size of two DG and slightly lesser than the sum of the size of three DG, as obtained in Table 4.7. A comparison between present work and the best available method is made for ELM. Simultaneously, from Table 4.8 it can be inferred that the minimum bus voltage is improved and reactive power

loss is minimized with the implementation of multiple DGs at different pfs as illustrated. The graphical representation of active power loss and reactive power loss for without DG, one DG, and multiple DGs are represented in Figure 4.5.

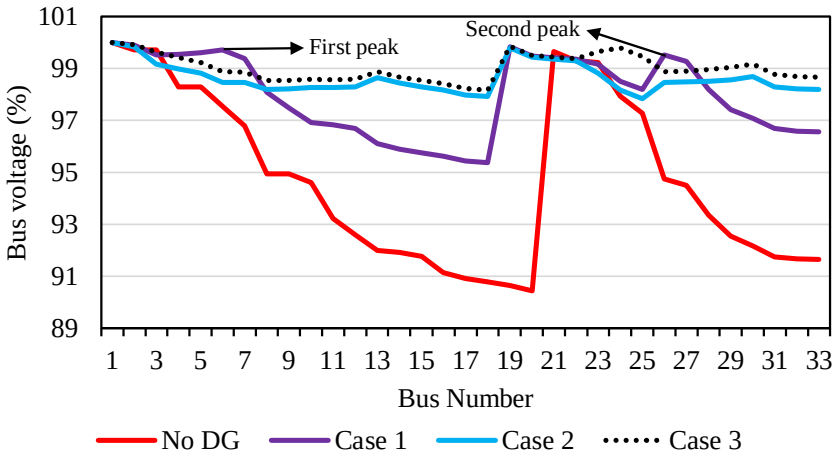

Figure 4.4: Voltage profile for 33 bus system considering WTG at 0.9 pf.

Table 4.7: Active power loss (MW) obtained considering WTG power factor

Reference	**pf**	**No DG**	**Case 1**	**Case 2**	**Case 3**
This Thesis	Unity	0.21101	0.11104	0.0727	0.05148
	0.85		0.06831	0.04539	0.02795
	0.82		0.06831	0.0444	0.02702
Active power loss obtained considering power factor of all conventional generations					
Reference	**pf**	**No CG**	**Single CG**	**Two CG**	**Three DG**
EA [225]	Unity	0.211	0.11107	0.087172	0.072787
	0.85		0.068170	0.03119	0.01552
	0.82		0.067870	0.03041	0.01514

Table 4.8: Minimum voltage, DG location, and reactive power loss (MVar) obtained

pf	Minimum Voltage (%)				reactive power loss			
	No DG	Case 1	Case 2	Case 3	No DG	Case 1	Case 2	Case 3
Unity		94.26	96.88	96.86		0.08168	0.05121	0.03848
0.85	90.44	95.74	98.12	98.15	0.14306	0.05504	0.03257	0.02185
0.82		96.0	98.20	98.22		0.05504	0.03195	0.02119

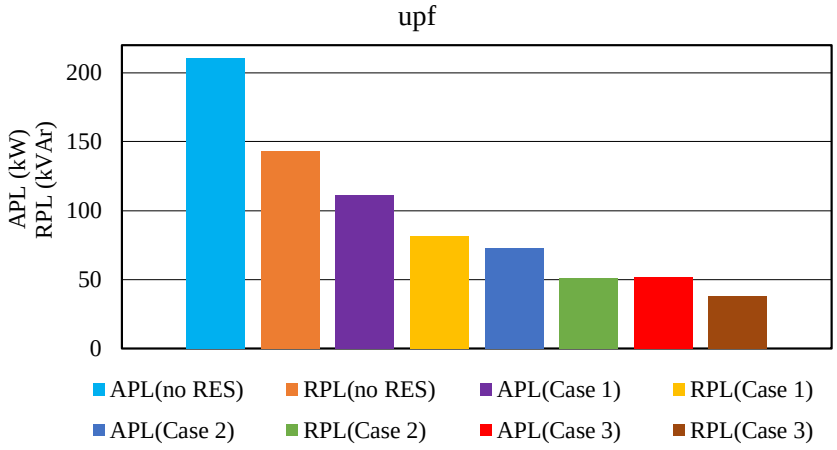

Figure 4.5: Active and Reactive Power Losses WTG at UPF.

4.4.3 Reliability Assessment

The indices obtained show the improvement in the system's reliability.[1] The indices are calculated for two different reliability data of DGs. It is observed that the indices are dependent on two reliability data, namely λ_p and RT of the system's elements. The present work has considered different reliability data for DG only. The best reliability improvement is observed for 0.2 of λ_p and 12 hr of RT. A detailed description of the DG reliability data effect on indices is given as per the following Scenarios.

- Scenario 1: 0.2 f/yr and 12 hr, as provided in Table 1.1
- Scenario 2: 0.4 f/yr and 12 hr
- Scenario 3: 0.6 f/yr and 12 hr

[1]Sachin Kumar, Kumari Sarita, Akanksha S.S. Vardhan, Rajvikram Elavarasan, R.K. Saket, Narottam Das, "Reliability Assessment of Wind-Solar PV Integrated Distribution System using Electrical Loss Minimization Technique", Energies. Vol. 13, No. 21, pp. 1-30 (2020)

- Scenario 4: 0.2 f/yr and 24 hr
- Scenario 5: 0.2 f/yr and 48 hr
- Scenario 6: No failure

Scenarios 1, 2, and 3 are considered by fixing the RT and varying λ_p. The appropriate case from the first three cases is then considered for variable RT to extract the best case from the top Five Scenarios. The values of DG reliability data (λ and RT) are being utilized to obtain the reliability indices for the system's reliability improvement. Equations (1.11) and (1.12) take these DG reliability data for further calculations. Furthermore, the following key assumptions are considered to assess the reliability of the EPDN.

- Circuit breakers, distribution lines, and potential transformers are available throughout with 100% reliability [226–228].
- The λ_p and RT of DG, Buses, feeders, and substations are given in Table 1.1.
- Load distribution and classification for 33 bus DS have been adapted from Appendix B Table B.2.

The authors in [226] have examined the failure rate of 0.0096 failure per year for 110 kV line. The high voltage lines are having low failure rate of approximately 0.02 failure per year, as mentioned in the [227]. The potential transformer has low failure rate of (1/29.29 =) 0.03 failure per year, as the time to first failure is given as 29.29 years in the [228]. Also, [7] has assumed the transformer to be 100% reliable.

A. Effect on Load-Oriented Indices

The EENS and AENS are obtained and tabulated in Tables 4.9 and 4.10 for all cases as illustrated in Figure 4.6–4.7, respectively. It is important to note that the EENS and AENS decrease with the number of DGs, and these are also decreased with decreasing values of λ_p and RT. As the increasing number of DGs are integrated into an EPDN, the supplied energy is improved in the EPDN, and thus, the indices related to the energy not supplied are reduced. This reduction is more while integrating the DGs with lesser λ_p and RT values. The reducing EENS and AENS are desirable, and thus, the EPDN reliability enhances with the integration of DGs with appropriate reliability data values.

Table 4.9: EENS (MWh per year) evaluated for different Scenarios

Case	Scenario 1	Scenario 2	Scenario 3	Scenario 4	Scenario 5	Scenario 6
No DG	82.763	82.763	82.763	82.763	82.763	82.763
Case 1	65.533	68.465	73.397	68.465	78.329	58.601
Case 2	31.817	29.249	31.817	29.249	34.385	24.113
Case 3	30.135	27.567	30.135	27.567	32.703	22.431

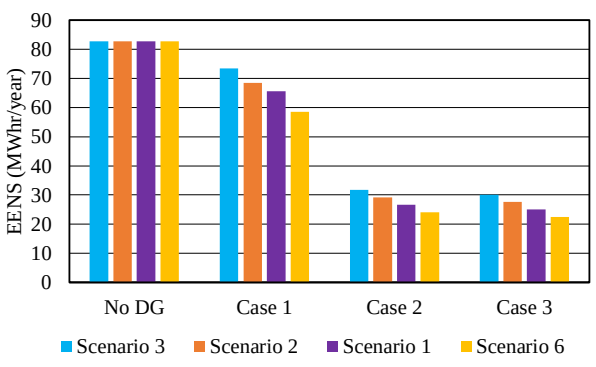

(a) EENS at different λ_p

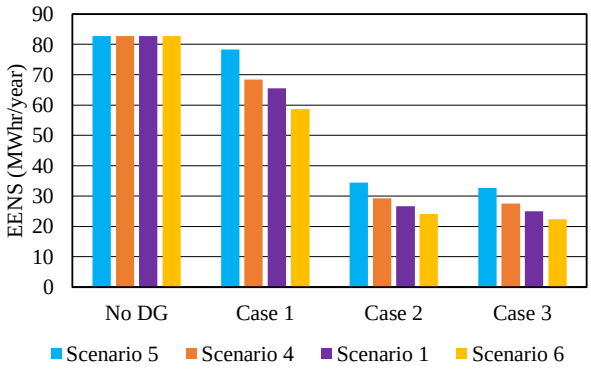

(b) EENS at different RT

Figure 4.6: EENS (MWh per year) obtained.

Table 4.10: AENS (MWh per customer per year) evaluated for different Scenarios

Case	Scenario 1	Scenario 2	Scenario 3	Scenario 4	Scenario 5	Scenario 6
No DG	0.0255	0.0255	0.0255	0.0255	0.0255	0.0255
Case 1	0.0196	0.0203	0.0226	0.0211	0.0241	0.0181
Case 2	0.0082	0.009	0.0098	0.009	0.0106	0.0074
Case 3	0.0077	0.0085	0.0093	0.0085	0.0101	0.0069

B. Effect on System-Oriented Indices

The SAIDI, and SAIFI are obtained and tabulated in Tables 4.11 and 4.12 for all cases considering all scenarios, as shown in Figure 4.8–4.9, respectively. The important point to be noted

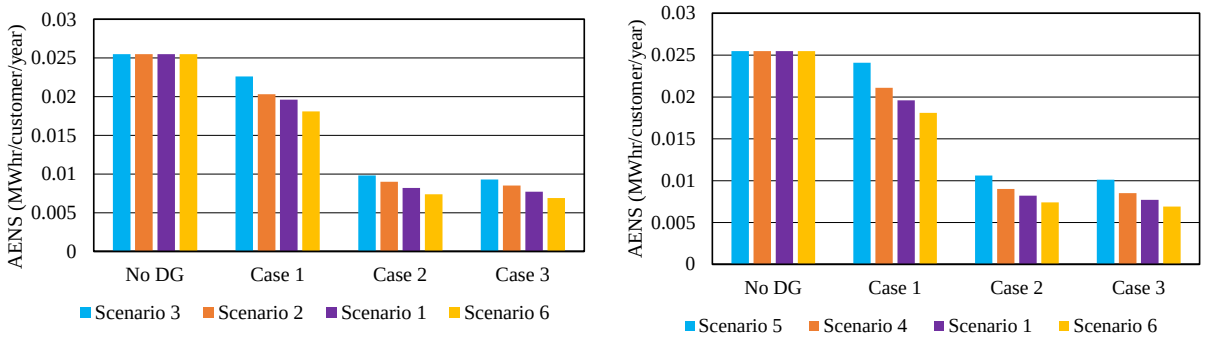

(a) AENS at different λ_p

(b) AENS at different RT

Figure 4.7: AENS (MWh per customer per year) obtained.

here that the SAIDI, and SAIFI, decreases with the increasing number of DGs; SAIDI is also decreased with the decreasing values of λ_p and RT. It is worthy to note that the SAIFI is not affected by the RT of the DG. It is because this index is independent of RT. As the increasing number of DGs are incorporated into the EPDN, the duration of the interruptions and the number of interruptions occurred in the customers' side are reduced. Thus, the SAIDI, and SAIFI are reduced. CAIDI can be determined using the ratio of SAIDI, and SAIFI. The reduction in the value of indices is more while integrating the DGs with lesser λ_p and RT values. Moreover, reducing SAIDI and SAIFI are desirable for EPDN reliability enhancement.

Table 4.11: SAIDI (hour per customer per year) evaluated for different Scenarios

Case	**Scenario 1**	**Scenario 2**	**Scenario 3**	**Scenario 4**	**Scenario 5**	**Scenario 6**
No DG	24.012	24.012	24.012	24.012	24.012	24.012
Case 1	18.764	20.085	21.406	20.085	22.728	17.442
Case 2	7.388	8.053	8.719	8.053	9.385	6.722
Case 3	7.201	7.866	8.532	7.866	9.198	6.535

The ASAI is determined and tabulated in Table 4.13 for all cases considering six scenarios as illustrated in Figure 4.10a and 4.10b. Due to the reduction in customers' interruption durations, the electrical power service availability for all loads or customers increases with the integration of multiple DGs. This index is further increased when DGs have a lower λ_p and RT values. The increment in ASAI increases leads to the decrement in ASUI, as incurred from Equations (1.25a) and (1.25c), which is desirable for the EPDN reliability improvement.

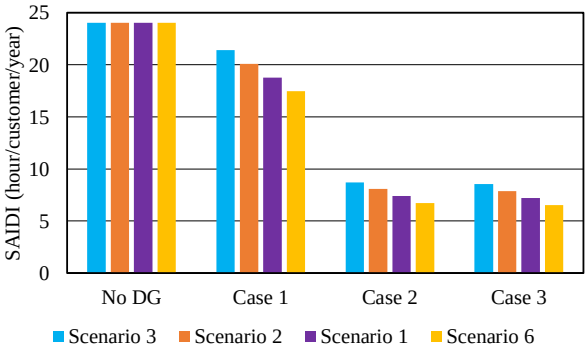

(a) SAIDI at different λ_p

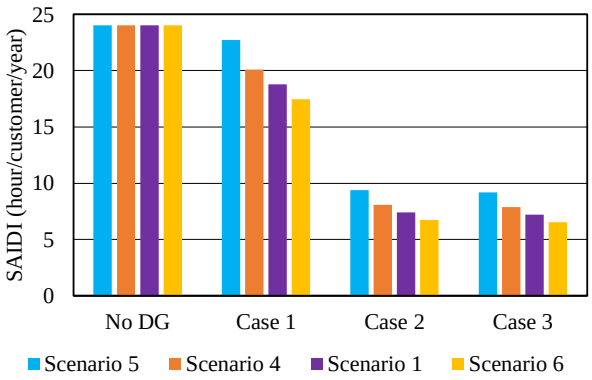

(b) SAIDI at different RT

Figure 4.8: SAIDI (hour per customer per year) obtained.

Table 4.12: SAIFI (failure per customer per year) evaluated for different Scenarios

Case	Scenario 1	Scenario 2	Scenario 3	Scenario 4	Scenario 5	Scenario 6
No DG	3.179	3.179	3.179	3.179	3.179	3.179
Case 1	2.109	2.219	2.329	2.109	2.109	1.999
Case 2	0.915	0.970	1.026	0.915	0.915	0.859
Case 3	0.842	0.897	0.953	0.842	0.842	0.786

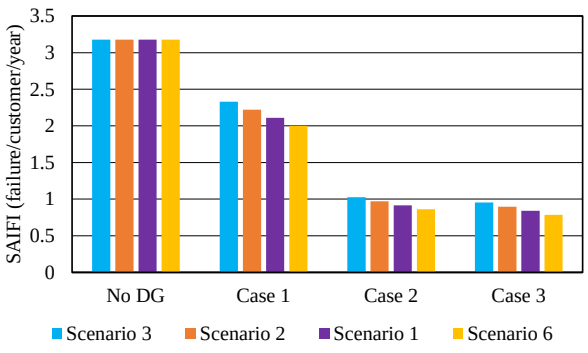

(a) SAIFI at different λ_p

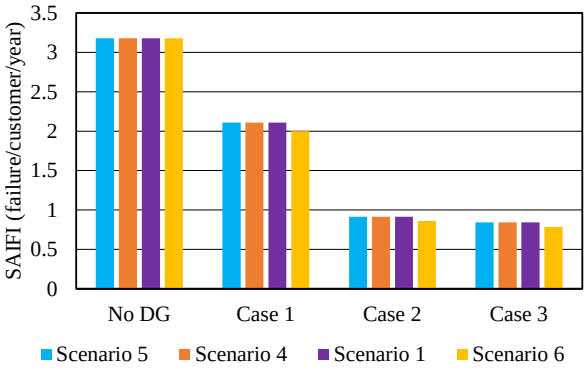

(b) SAIFI at different RT

Figure 4.9: SAIFI (failure per customer per year) obtained.

4.5 Summary

The earlier work performed on reliability assessment of distribution system has been extended and described in this chapter. Three RESs were considered: WTG, SPV, and BESD integrated into DS of 33 bus. The manufacturers' specifications, mainly the power ratings of the three

Table 4.13: ASAI (pu) evaluated for different Scenarios

Case	Scenario 1	Scenario 2	Scenario 3	Scenario 4	Scenario 5	Scenario 6
No DG	0.99726	0.99726	0.99726	0.99726	0.99726	0.99726
Case 1	0.99786	0.99771	0.99756	0.99771	0.99741	0.99801
Case 2	0.99916	0.99908	0.99900	0.99908	0.99893	0.99923
Case 3	0.99918	0.99910	0.99903	0.99910	0.99895	0.99925

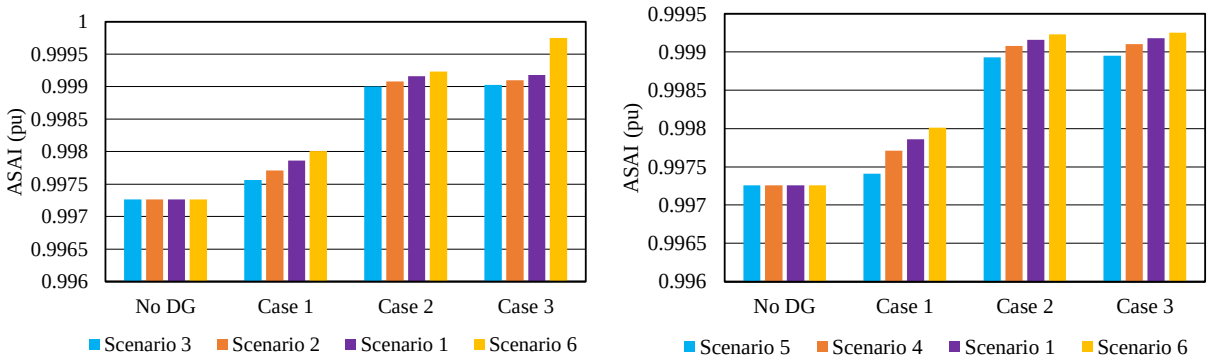

(a) ASAI at different λ_p

(b) ASAI at different RT

Figure 4.10: ASAI (pu) obtained.

RESs, were considered for optimizing the ratings. As WTG and SPV are highly prone to failures due to multiple assemblies and components, therefore, the Failure Rate and Repair Time of WTG and SPV were assumed to be greater than the previously explained conventional generations, as mentioned in [229, 230]. In contrast, it is assumed that the BESD is 100% reliable and fully charged.

Further, the minimized active power loss (0.02702 MW) and reactive power loss (0.02119 MVar) with better minimum voltage (98.22%) are obtained when compared to [225]. Finally, the following values have been evaluated for the excellent reliability of the test system.

For 33 bus system:

EENS: 22.431 MWh per year

AENS: 0.0069 MWh per customer per year

SAIDI: 6.535 hour per customer per year

SAIFI: 0.786 failure per customer per year

ASAI: 0.99925 per unit

The reliability of the IEEE 33 and 118 bus systems when coupled with conventional and wind power is discussed in the next chapter. The use of energy sources with optimal placements and ratings has been found to enhance the test system's reliability at a lower cost per year.